In-vitro Virucidal Activity of Hypothiocyanite and Hypothiocyanite/lactoferrin Mix Against SARS-CoV-2

Luca Cegolon (l.cegolon@gmail.com)
Local Health Unit N.2 "Marca Trevigiana", Public Health Department, Treviso, Italy
Mattia Mirandola
Padua University, Department of Molecular Medicine, Padua, Italy
Claudio Salaris
Padua University, Department of Molecular Medicine, Padua, Italy
Maria Salvati
Padua University, Department of Molecular Medicine, Padua, Italy
Cristiano Salata
Padua University, Department of Molecular Medicine, Padua, Italy
Giuseppe Mastrangelo
Padua University, Department of Cardiac, Thoracic, Vascular Sciences, & Public Health, Padua, Italy

Research Article

Keywords: Hypothiocyanite, Lactoferrin, Lactoperoxidase system, ALX-009, SARS-CoV-2, COVID-19

Posted Date: December 29th, 2020

DOI: https://doi.org/10.21203/rs.3.rs-131956/v1

Abstract

SARS-CoV-2 replicates efficiently in the upper airways during the prodromal stage, with resulting viral shedding into the environment from patients with active COVID-19 as well as from asymptomatic individuals. There is a need to find pharmacological interventions to mitigate the spread of COVID-19. Hypothiocyanite and lactoferrin are molecules of the innate immune system with a large spectrum cidal activity and easy to administer by aerosol inhalation. The combination of the above two molecules was designated as orphan drug by the Food and Drug Administration and the European Medicines Agency. Here we found a dose-dependent as well as time-dependent virucidal activity of hypothiocyanite at micromolar concentrations, slightly improved by lactoferrin, against SARS-CoV-2. The two substances individually tested were devoid of any cytotoxicity.

Background

SARS-CoV-2 enter cells through the angiotensin-converting enzyme 2 (ACE2) membrane receptor, widely expressed in human airways, particularly by epithelial cells of the nasal cavity and by type II epithelial cells of pulmonary alveoli [1, 2]. On the other hand, COVID-19 physiopathology can be broken down by three clinical stages, depending on the main site of the infection [3]. At initial asymptomatic stage COVID-19 is predominantly located in the nasal cavity, which triggers a contained local innate immune response. In mild symptomatic stage, COVID-19 mainly affects the pseudostratified epithelium of the upper respiratory tract, which can recover because its basal cells are spared. COVID-19 may be more severe in smaller (lower) branches of the bronchial airways, where club cells are likely infected. In the third (life-threatening) stage, SARS-CoV-2 spreads into pulmonary alveoli, infecting type II epithelial cells expressing the ACE2 receptor.

Whilst treatment options for patients with severe disease requiring hospitalization are now available, with corticosteroids emerging as treatments of choice for critically ill COVID-19 patients [4], there is a noteworthy lack of effective remedies against mild to moderate disease. Treatments with few adverse effects and easy to administer in outpatient settings, combined with an effective vaccine, could end the ongoing COVID-19 pandemic [5]. Molecules derived from the innate immune system, such as hypothiocyanite ($OSCN^-$; structural formula $^-O\text{-}S\text{-}C \equiv N$) and lactoferrin (LF), can represent promising candidates due to their broad-spectrum antimicrobial and antiviral activity [6, 7].

In view of the above, we conducted an in-vitro study on $OSCN^-$ and a combination of $OSCN^-$ and LF, with the aim of testing their virucidal activity and cytotoxicity.

Methods

Cell culture and viruses

Vero (African green monkey kidney cells, ATCC® CCL-81), Vero E6 (ATCC® CRL1586) and HEK293T (ATCC® CRL-11268TM) cells were grown in Dulbecco's modified Eagle's medium (D-MEM) containing 10% heat-inactivated fetal bovine serum (FBSi). Cells were maintained in a 5% CO2 incubator at 37 °C, routinely checked for mycoplasma and confirmed negative. Culture medium and FBSi were obtained from Gibco (Thermofisher).

SARS-CoV-2 (Genbank: MW000351) and the rVSVΔG-Luc, a recombinant Vesicular Stomatitis Virus containing the gene encoding for the luciferase protein in place of the VSV-G gene [8], were used in the experiments.

Virus stock preparation and titration

Vero E6 cells were seeded in T175 flasks and then infected with SARS-CoV-2 (MOI of ≈ 0.1). At 72–96 h post infection (p.i.), supernatants were collected, centrifuged at 2,300 rpm for 10 min, then stored in aliquots at -80 °C. Viral titer was determined by plaque assay on Vero E6 cells seeded on 24-well plates. Tenfold virus dilutions were prepared in DMEM and inoculated on confluent Vero-E6 cells for 1 h at 37 °C. After that, virus inoculum was removed from each well and cells were overlaid with 300 µL of 0.6% carboxymethylcellulose (Merck) diluted in DMEM supplemented with 2% FBSi. Seventy-two h p.i., cells were fixed adding 300 µL of 5% formaldehyde (Merck) in PBS 1x for 30 min at room temperature. Then, cells were stained with crystal violet in 20% ethanol. Virus titer was measured as plaque-forming units per milliliter (PFU/mL) based to the plaques formed in cell culture upon infection. All studies with viable SARS-CoV-2 were performed in the certified BSL3 laboratory.

For SARS-CoV-2-pseudotyped VSV production (rVSV-S), HEK293T cells were seeded in T175 flasks and then transfected by calcium phosphate-DNA precipitation with 40 µg of pSARS-CoV-2-spike plasmid. After 24 h, cells were infected with the rVSVΔG-Luc virus at the multiplicity of infection (MOI) of 4 fluorescent focus-forming units (FFU)/cell. Sixteen hours p.i., cell culture supernatants were harvested and cell debris were cleared by centrifugation (2,300 rpm for 7 minutes at 4 °C). Then, virus particles were pelleted by ultracentrifugation on a 20% p/v a sucrose cushion (27,000 rpm for 150 min at 4 °C) in a Beckmann SW 28 Ti Swinging-Bucket rotor. Pellets were resuspended in 1 mL of ice-cold PBS1X / tube and mixed. Subsequently, the virus was aliquoted and stored at -80 °C until use.

Titration of virus was determined by immunofluorescence on Vero cells seeded on 96-well plates. Viral stock was tenfold serially diluted in DMEM and inoculated on confluent Vero cells for 1 h at 37 °C. Then, cells were washed and DMEM supplemented with 10% FBSi was added. After 18 h, cells were fixed with precooled methanol-acetone for 1 h at -20 °C. Immune staining was performed by incubation with 1:3000 anti-VSV-M [23H12] monoclonal antibody (Kerafast) on the infected cells for 90 minutes at 37 °C, followed by incubation with 1:1000 anti-rabbit Alexa Fluor® 488 (Thermo Fisher Scientific) for 60 minutes at 37 °C. The fluorescent foci in each well were counted and viral titer was expressed as FFU/mL [9].

Compounds preparation and cytotoxicity assay

$OSCN^-$ solution was prepared via enzymatic reaction with an automated equipment EOLEASE® (Alaxia, Lyon, France). Due to its intrinsic reactivity, each solution freshly prepared was used alone or combined with Lactoferrin within 15 min after preparation. Reagents for the $OSCN^-$ production were provided by Alaxia.

Pharma-grade lyophilized Lactoferrin (purity > 98%) was made available by Alaxia, as sterile vials. Lyophilized Lactoferrin was reconstituted as solution with 0.9% sodium chloride solution at 10 g/L.

Compound dilutions for virus treatment were performed in Minimum Essential Media (MEM) purchased by Gibco.

Cytotoxicity of $OSCN^-$ and LF was determined on Vero and Vero-E6 cells after 24 h of treatment. Cell viability was tested with an assay based on the reduction of a tetrazolium salt (MTT Cell Proliferation Assay, Thermofisher) in a 96-well plate format according to the manufacturer's instructions.

Virucidal assay

To evaluate the OSCN- and LF virucidal activity, 4×10^4 FFU of rVSV-S were incubated for 1 h at 37 °C with 0–3.125–6.25–12.5–25–50 and 100 µM of OSCN- with or without 4 g/L of LF. Positive control (mock sample) was treated with the solution used to prepare the $OSCN^-$ simulating the max $OSCN^-$ concentration. Next, Vero cells seeded on 96-well plates were infected for 1 h at 37 °C. Eighteen hours later, infection was evaluate measuring the relative light unit (RLU) with a VICTOR Multilabel Plate Reader (PerkinElmer) using the Steady-Glo® Luciferase Assay System (Promega).

In the case of SARS-CoV-2, 1×10^5 PFU were incubated for 1 h at 37 °C with 0–6.25–12.5–25–50 and 100 µM of $OSCN^-$ with or without 4 g/L of LF. Next, tenfold virus dilutions were prepared in MEM and processed as above reported for the plaque assay. Viral titer was calculated for each sample and the virucidal activity was measured evaluating the efficiency of the infection in comparison to the mock treated control.

Statistical analysis

All the experiments were performed in duplicate in at least three independent biological replicates. Statistical analysis was carried out with GraphPad Prism software package, employing the one-way ANOVA test. The threshold for statistical significance was $P < 0.05$. All details on sample size and P values for each experiment are provided in the relevant figure or its legend. Curve fitting was performed to determine IC_{50} values using a sigmoidal 4PL model in GraphPad Prism 8 software.

Results

Virucidal activity of $OSCN^-$ and $OSCN^-$/LF

The virucidal activity of $OSCN^-$ was firstly investigated with a recombinant Vesicular Stomatitis Virus (rVSV), encoding the reported gene luciferase instead of the viral glycoprotein. The rVSV can be easily manipulated under biosafety level 2 conditions and pseudotyped by the S protein obtaining a virus (rVSV-S) with a tropism dictated by the heterologous S envelope which represents an excellent surrogate of SARS-CoV-2 to study the virus entry and the viral neutralization [8, 10, 11]. Indeed, rVSV-S was incubated with different $OSCN^-$ concentrations for 60 min at 37 °C (pre-treatment), and then Vero cells were infected at multiplicity of infection (MOI) 0.065 FFU/cell. Sixteen hours post infection, cells were lysed and the luciferase expression was evaluated as a measure of viral infection. As shown in Fig. 1a, viral infection is inhibited in a dose-dependent manner and the concentration capable of reducing the viral infectivity by 50% (IC_{50}) was 4.64 μM. Figure 1b shows that the efficacy of the virucidal activity of $OSCN^-$ was clearly time-dependent in all conditions tested (pre-treatment, 60, 40 or 20 minutes or co-treatment – 0 minutes - adding $OSCN^-$ during the infection of target cells). We observed a reduction of the viral infectivity of more than 50% until the concentration of 6.25 μM (Fig. 1b), when the rVSV-S was incubated with $OSCN^-$ before the infection. In case of co-treatment, a reduction of virus infectivity higher than 50% was observed starting from $OSCN^-$ concentration of 12.5 μM.

We also investigated the virucidal activity of $OSCN^-$ and LF combination. Preliminary experiments with LF showed that concentrations higher than 1 g/L were required to inhibit the viral infection (data not shown). Then, we selected a concentration of 4 g/L that was close to that previously used with $OSCN^-$ in experiments against bacteria [12]. The combination $OSCN^-$/LF significantly increased the virucidal activity using lower doses of $OSCN^-$, achieving an inhibition of viral infection > 90% in comparison to 80–85% with $OSCN^-$ alone (Fig. 1c) or 25% with LF alone (data not shown). These data suggest that, in our experimental conditions, $OSCN^-$ has the main virucidal effect, whereas at lower $OSCN^-$ concentrations LF can contribute improving virus inactivation. Since the addition of $OSCN^-$ and LF was not toxic to Vero cells, monitored for 24 h by the MTT test, the inhibition of the viral infectivity was due to the interference of the compounds on the capacity of the virus to infect cells (Fig. 2).

Finally, to validate the results obtained with the rVSV-S, we performed experiments with $OSCN^-$ and $OSCN^-$/LF using SARS-CoV-2. After virus-compound incubation for 60 min, tenfold dilutions of virus-compound mix were inoculated on Vero-E6 cells (used for virus isolation and propagation) and the reduction of plaque generation was evaluated. Results reported in Fig. 3 confirmed the dose-dependent virucidal activity of $OSCN^-$ (Fig. 3a) and demonstrated that higher doses of $OSCN^-$ are effective to inhibit SARS-CoV-2 infection also with an incubation of 20 min (Fig. 3b). In contrast to rVSV-S, the enhancement of the virucidal activity of $OSCN^-$ was less pronounced for SARS-CoV-2 in presence of LF (Fig. 3c).

Overall, our results indicate that $OSCN^-$ has a strong virucidal activity against SARS-CoV-2, the combination of $OSCN^-$/LF further improved the virucidal effect of $OSCN^-$ by moderate margin and, lastly, hypothiocyanite and LF were not toxic to Vero cells.

Discussion

We evaluated the virucidal activity of $OSCN^-$ and $OSCN^-$/LF against SARS-CoV-2. In our experimental conditions, $OSCN^-$ had the main virucidal effect in-vitro against SARS-CoV-2. Three components are mixed in airway lumen to produces this biocidal compound: the enzymatically active lactoperoxidase (LPO), secreted by serous cells of the submucosal glands and by goblet cells; the anion thiocyanate (SCN^-), delivered by duct cells of submucosal gland; and hydrogen peroxide (H_2O_2), made by epithelial cells [13]. Unlike in the trachea, the main bronchi, third and fifth generation bronchi, LPO mRNA was nearly absent in lung parenchyma suggesting absence of $OSCN^-$ production in the alveoli [14]. Furthermore, due to the need of enhancing gas exchange, epithelial alveolar cells cannot contain strong protective structures and hence are weak, fragile and more vulnerable to viral attacks. The biocidal effect of $OSCN^-$ takes place in the airways lumen. Interestingly, it was found that a solution of the two molecules combined (ALX-009, developed by Alaxia SAS for the treatment of bacterial infection in cystic fibrosis patients [15]) was easily administered by inhalation of aerosol, using a nebulizer as delivery device, in a Phase I Clinical Trial (NCT02598999 of 2018) to healthy volunteers and patients affected by cystic fibrosis. Thereafter, on May 2009, the combination of $OSCN^-$ and LF for treatment of cystic fibrosis was designated as orphan drug by the US Food and Drug Administration and the European Medicines Agency [15]. Topical administration of $OSCN^-$ and LF combined, in the form of aerosol, might effectively inactivate free SARS-CoV-2 virions nearing the epithelium from outside or released from infected cells, thus mitigating or preventing the spread of the infection in the host tissues as well as its propagation to further susceptible individuals.

Despite strong evidence of SARS-CoV-2 inactivation, the exact virucidal mechanism of $OSCN^-$ is still unknown. Ozone at high doses has been shown to inactivate SARS-CoV-2 by oxidative stress both directly and indirectly through reactive oxygen species produced by ozone decomposition and/or by oxidation of double bonds of viral lipids, proteins, and amino acids that lead to the formation of reactive radicals (RCOO·) [16]. Indirect modes of action further propagate the oxidation through a chain reaction [17]. Enveloped viruses - as vesicular stomatitis Indiana virus, vaccinia virus, influenza A virus and certain strains of type 1 herpes simplex virus - are more sensitive to ozone, whereas non-enveloped adenovirus type 2 was more resistant to this gas [18; 19]. Irreversible oxidative damage of the lipid components of the viral envelope or the nucleoproteins could also be the mechanism of virucidal activity against SARS-CoV-2 of $OSCN^-$, which is a less potent (but also less damaging) oxidizing agent than ozone. As already shown, LPO gives $OSCN^-$ in presence of SCN^-; $OSCN^-$ in turn reacts with the thiol moiety of peptides or proteins (R-SH) generating sulfenyl thiocyanate (R-S-SCN), which by adding one molecule of H_2O produces sulfenic acid (R-S-OH) as well as SCN^- at the end of the cycle [7]. The LPO cycle thus extends the duration of effects of $OSCN^-$ beyond the limited half-life (about 1 hour) of this compound [20]. Sulphydryl oxidation determines inhibition of numerous enzymes if the proteins contain the amino acid cysteine, which is abundant in the coronavirus proteins such as those in the spikes of the envelope [17].

The $OSCN^-$ concentration used in our experimental conditions was up to 100 μM, higher than that reported in human saliva (20–60 μM) or in resting (31 μM), stimulated whole saliva (25 μM) and parotid saliva (30 μM), respectively [21, 22]. Our data suggested that physiological $OSCN^-$ concentrations could inhibit at least the 50% of SARS-CoV-2 infection. However, $OSCN^-$ and bovine LF concentrations in ALX-009 were higher than those used in our experimental setting, reaching values of 3,600 μM and 8 g/L respectively, which therefore should likely maximize their respective virucidal activity [12].

Moreover, we have previously demonstrated that $OSCN^-$ inhibits A(H1N1)pdm09 influenza virus infection, when the virus was challenged with $OSCN^-$ for 60 min at 37 °C before infection, with a similar IC_{50} than the one determined for rVSV-S [23]. Thereafter the antiviral activity of $OSCN^-$ was tested also against several other types of influenza virus, confirming a strain independent virucidal effect [24; 25]. Overall, these results indicate a potent and potentially wide-range antiviral activity of $OSCN^-$.

Lactoferrin, one of the most abundant antimicrobial proteins in normal airway secretions [15], seems to improve the inhibition of the viral infection only at lower $OSCN^-$ concentrations. The antiviral mechanism of LF is based on the ability to prevent the virus from anchoring with targeted cells [26]. In particular, LF binds with heparan sulfate proteoglycans (HSPGs), which are cell-surface and extracellular matrix macromolecules acting as an attachment factor for many viruses including SARS-CoV-1. LF blocks the infection of SARS-CoV-1 by competing with the virus for HSPGs, therefore preventing the viral concentration on the surface of target cells [26]. Given this mechanism of action, the antiviral activity of LF could be better displayed with an in-vivo study.

In conclusion, our results indicate that $OSCN^-$ and LF have a virucidal activity against SARS-CoV-2, alone or in combination. Although the in vitro results require an in-vivo validation, the LF and $OSCN^-$ combination may have a relevant clinical impact reducing the diffusion of infection in the host tissues as well as the spread of SARS-CoV-2 particles to new susceptible hosts. The latter, can have important positive effects to control the COVID-19 pandemic.

Declarations

Acknowledgements

We are grateful to Alaxia SAS that provided protocols, equipment and reagents to prepare $OSCN^-$ and LF. We thank Michael Whitt, University of Tennessee, Memphis, USA, for providing the VSVΔG-Luc and Maria Rita Gismondo, L. Sacco University Hospital, Milan, Italy, for providing the SARS-CoV-2.

Competing interests

Authors did not accept honoraria or other payments from Alaxia or other pharmaceutical industries. No other conflicts of interest have to be declared.

Funding

This work was supported by University of Padova grants (DOR-2019-2020 to CrS).

References

1. Salata, C., Calistri, A., Parolin, C., Palù, G., 2019a. Coronaviruses: a paradigm of new emerging zoonotic diseases. Pathog. Dis. 77(9), ftaa006. (2019).
2. Yao, Y., Wang, H., Liu, Z. Expression of ACE2 in airways: Implication for COVID-19 risk and disease management in patients with chronic inflammatory respiratory diseases. Clin. Exp. Allergy (2020).
3. Mason, R.J. Thoughts on the alveolar phase of COVID-19. Am. J. Physiol. Lung. Cell. Mol. Physiol. 319(1), L115-L120 (2020).
4. Prescott, H.C., Rice, T.W. Corticosteroids in COVID-19 ARDS: evidence and hope during the pandemic. JAMA. 324(13), 1292-1295 (2020).
5. Kim, P.S., Read, S.W., Fauci, A.S., 2020. Therapy for Early COVID-19: A Critical Need. JAMA. 324(21), 2149-2150 (2020).
6. Cegolon, L. Investigating hypothiocyanite against SARS-CoV-2. Int. J. Hyg. Environ. Health. 227, 113520 (2020).
7. Cegolon, L., Javanbakht, M., Mastrangelo, G., Nasal disinfection for the prevention and control of COVID-19: A scoping review on potential chemo-preventive agents. J. Hyg. Environ. Health. 230, 113605 (2020).
8. Whitt, M.A. Generation of VSV pseudotypes using recombinant ΔG-VSV for studies on virus entry, identification of entry inhibitors, and immune responses to vaccines. J. Virol. Methods. 169(2), 365-74 (2010).
9. Salata, C., Baritussio, A., Munegato, D., Calistri, A., Ha, H.R., Bigler, L., Fabris, F., Parolin, C., Palu', G., Mirazimi, A. Amiodarone and metabolite MDEA inhibit Ebola virus infection by interfering with the viral entry process. Dis. 73(5), ftv032 (2015).
10. Nie, J., Li, Q., Wu, J., Zhao, C., Hao, H., Liu, H., Zhang, L., Nie, L., Qin, H., Wang, M., Lu, Q., Li, X., Sun, Q., Liu, J., Fan, C., Huang, W., Xu, M., Wang, Y. Quantification of SARS-CoV-2 neutralizing antibody by a pseudotyped virus-based assay. Nat. Protoc. 15(11), 3699-3715 (2020).
11. Salata, C., Calistri, A., Alvisi, G., Celestino, M., Parolin, C., Palù, G. Ebola Virus Entry: From Molecular Characterization to Drug Discovery. Viruses. 11(3), 274 (2019).
12. Tunney, M.M., Payne, J.E., McGrath, S.J., Einarsson, G.G., Ingram, R.J., Gilpin, D.F., Juarez-Perez, V., Elborn, J.S. Activity of hypothiocyanite and lactoferrin (ALX-009) against respiratory cystic fibrosis pathogens in sputum. J. Antimicrob. Chemother. 73(12), 3391-3397 (2018).
13. Conner, G.E., Salathe, M., Forteza, R. Lactoperoxidase and hydrogen peroxide metabolism in the airway. Am. J. Respir. Crit. Care. Med. 166(12 Pt 2), S57-61 (2002).

14. Gerson, C., Sabater, J., Scuri, M., Torbati, A., Coffey, R., Abraham, J.W., Lauredo, I., Forteza, R., Wanner, A., Salathe, M., Abraham, W.M., Conner, G.E. The lactoperoxidase system functions in bacterial clearance of airways. Am. J. Respir. Cell. Mol. Biol. 22(6), 665-71 (2000).
15. Moreau-Marquis, S., Coutermarsh, B., Stanton, B.A. Combination of hypothiocyanite and lactoferrin (ALX-109) enhances the ability of tobramycin and aztreonam to eliminate Pseudomonas aeruginosa biofilms growing on cystic fibrosis airway epithelial cells. J. Antimicrob. Chemother. 70(1), 160-6 (2015).
16. Rowen, R.J., Robins, H., 2020. A plausible “penny” costing effective treatment for corona virus - ozone therapy. Infect. Dis. Epidemiol. 6, 113 (2020).
17. Tizaoui, C. Ozone: A Potential Oxidant for COVID-19 Virus (SARS-CoV-2). Ozone: Science & Engineering. 42(5), 378-385 (2020).
18. Gavazza, A., Marchegiani, A., Rossi, G., Franzini, M., Spaterna, A., Mangiaterra, S., Cerquetella, M. Ozone Therapy as a Possible Option in COVID-19 Management. Front. Public. Health. 8, 417 (2020).
19. Murray, B.K., Ohmine, S., Tomer, D.P., Jensen, K.J., Johnson, F.B., Kirsi, J.J., Robison, R.A., O'Neill, K.L. Virion disruption by ozone-mediated reactive oxygen species. J. Virol. Methods. 153(1), 74-7 (2008).
20. Ashby, M.T., Kreth, J., Soundarajan, M., Sivuilu, L.S. Influence of a model human defensive peroxidase system on oral streptococcal antagonism. Microbiology (Reading). 155(Pt 11), 3691-3700 (2009).
21. Jalil, RA. Concentrations of thiocyanate and hypothiocyanite in the saliva of young adults. Nihon. Univ. Sch. Dent. 36(4), 254-60 (1994).
22. Tenovuo, J. Clinical applications of antimicrobial host proteins lactoperoxidase, lysozyme and lactoferrin in xerostomia: efficacy and safety. Oral Dis. 8(1), 23-9 (2002).
23. Cegolon, L., Salata, C., Piccoli, E., Juarez, V., Palu', G., Mastrangelo, G., Calistri, A. In vitro antiviral activity of hypothiocyanite against A/H1N1/2009 pandemic influenza virus. Int. J. Hyg. Environ. Health. 217, 17-22 (2014).
24. Gingerich, A., Pang, L., Hanson, J., Dlugolenski, D., Streich, R., Lafontaine, E.R., Nagy, T., Tripp, R.A., Rada, B. Hypothiocyanite produced by human and rat respiratory epithelial cells inactivates extracellular H1N2 influenza A virus. Inflamm. Res. 65(1), 71-80 (2016).
25. Patel, U., Gingerich, A., Widman, L., Sarr, D., Tripp, R.A., Rada, B., 2018. Susceptibility of influenza viruses to hypothiocyanite and hypoiodite produced by lactoperoxidase in a cell-free system. PLoS One. 13(7), e0199167 (2018).
26. Lang, J., Yang, N., Deng, J., Liu, K., Yang, P., Zhang, G., Jiang, C., 2011. Inhibition of SARS pseudovirus cell entry by lactoferrin binding to heparan sulfate proteoglycans. PLoS One. 6(8), e23710.

Figures

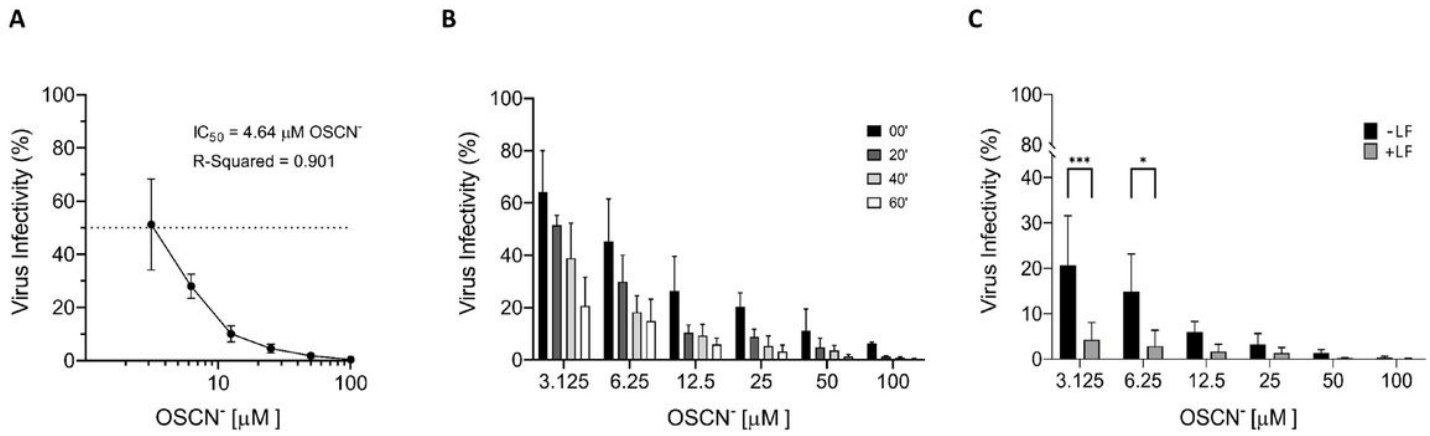

Figure 1

OSCN- and OSCN-/LF virucidal activity against the pseudovirus VSV-S. (A) Efficiency of pseudovirus infection after exposition at different OSCN- concentrations for 1 h at 37 °C. (B) Evaluation of the virucidal activity of OSCN- after pseudovirus treatment for 0, 20, 40, and 60 min at 37 °C before the infection of target cells. (C) Comparison between OSCN- and OSCN-/LF virucidal activity after 1 h of pretreatment of VSV-S before cells infection. Data (mean ± SD, N = 3, experiments in duplicate) are percentages of no drug, set as 100% (* = P < 0.05; *** = P < 0.001).

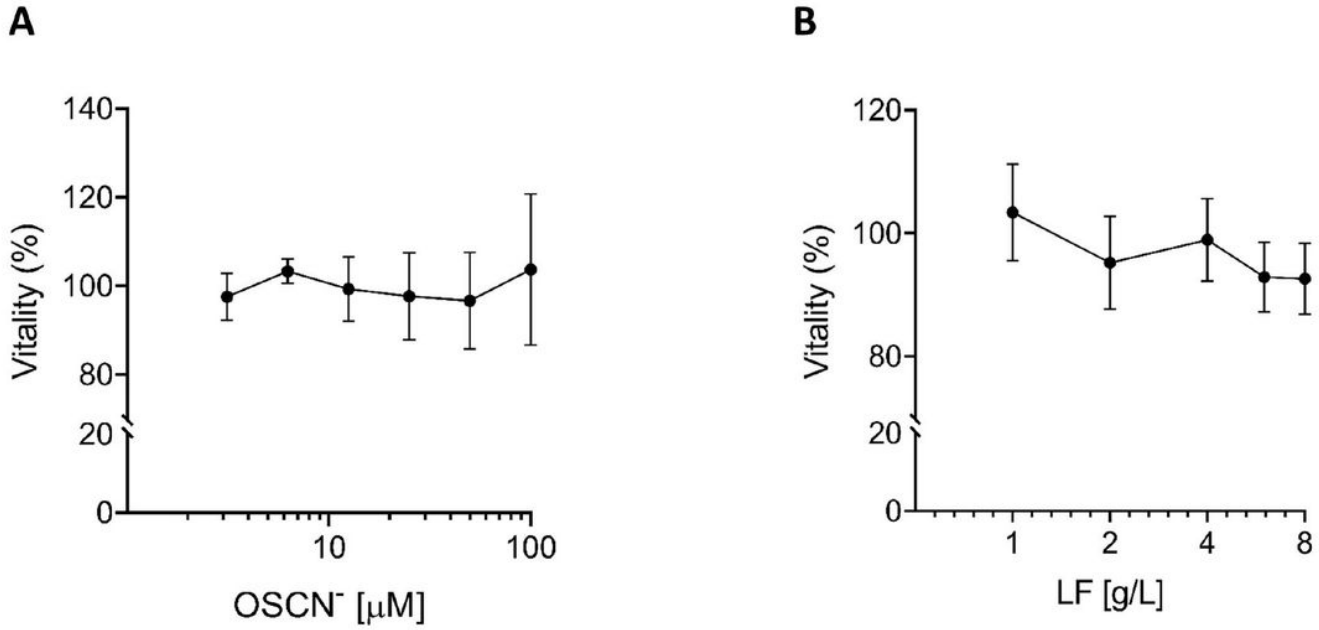

Figure 2

Cytotoxicity of OSCN- and LF. The cytotoxicity of (A) OSCN- and (B) LF was evaluated on Vero cells after 24 h of treatment using the MTT assay. Data (mean ± SD, N = 3, experiments in quadruplicate) are percentages of no drug, set as 100%.

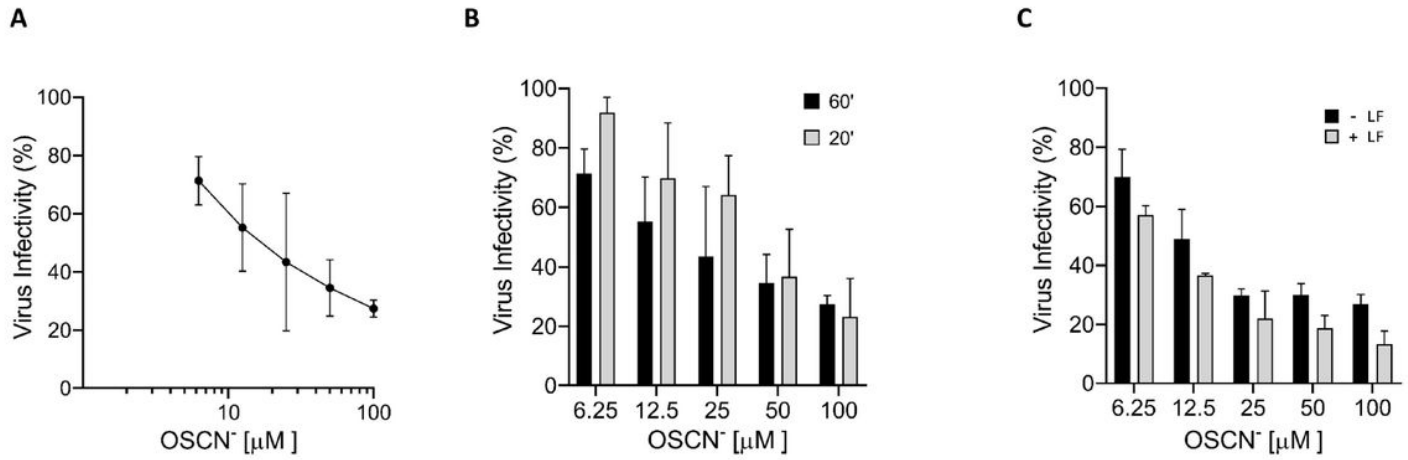

Figure 3

Virucidal activity of OSCN- and OSCN-/LF against SARS-CoV-2. SARS-CoV-2 was treated for 1 h at 37 °C with OSCN- alone or supplemented with LF before infection of cells. The reduction of infectivity was evaluated by plaque assay. (A) virucidal effect of OSCN-. (B) Comparison between different times of virus-OSCN- exposition on the efficiency of the virucidal activity. (C) Evaluation of the combination OSCN-/LF on the virucidal activity. Data (mean ± SD, N = 3, experiments in duplicate) are percentages of no drug, set as 100%.